AD-A126 818 EXPERIMENTAL INVESTIGATION OF AERODYNAMIC WINDOWS(U) 1/1
FOREIGN TECHNOLOGY DIV WRIGHT-PATTERSON AFB OH
18 FEB 83 FTD-ID(RS)T-1813-82

UNCLASSIFIED F/G 20/6 NL

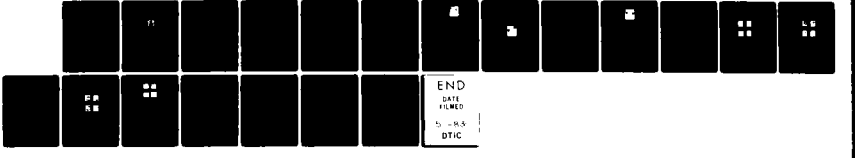

END
DATE FILMED
5-83
DTIC

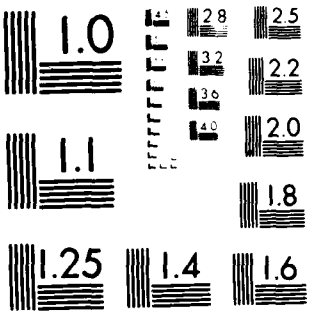

FTD-ID(RS)T-1813-82

FOREIGN TECHNOLOGY DIVISION

EXPERIMENTAL INVESTIGATION OF AERODYNAMIC WINDOWS

EDITED TRANSLATION

FTD-ID(RS)T-1813-82 18 February 1983

MICROFICHE NR: FTD-83-C-000240

EXPERIMENTAL INVESTIGATION OF AERODYNAMIC WINDOWS

English pages: 16

Source: Jiguang, Vol. 7, Nr. 10, 1980, pp. 7-12

Country of origin: China
Translated by: LEO KANNER ASSOCIATES
F33657-81-D-0264
Requester: FTD/TQTD

PREPARED BY:

TRANSLATION DIVISION
FOREIGN TECHNOLOGY DIVISION
WP-AFB, OHIO.

GRAPHICS DISCLAIMER

All figures, graphics, tables, equations, etc. merged into this translation were extracted from the best quality copy available.

EXPERIMENTAL INVESTIGATION OF AERODYNAMIC WINDOWS

Group 105, Shanghai Institute of Optics and Fine Mechanics, Academia Sinica

Abstract

This paper desribes the design and experiments of three types of aerodynamic windows: the expansion window, compression window and vortex window. These three windows have apertures of 3 cm and were designed to operate at cavity pressures of 0.1 atm. When the beam passes through the window, the minimum beam degradation is 1.5 times as large as the diffraction limit of the aperture. The minimum mass flow required for the operation of the window is 0.012 kg/sec · cm^2.

Introduction

When using laser beams from common solid windows with high energy density output in a high energy gas laser, because the window material produces serious thermal effects, the output is seriously distorted and even causes window breaking. Therefore, the aerodynamic window is presently already used as the output window of high energy lasers and has been applied in actual devices.

This paper describes the design and experiments of several types of aerodynamic windows: the expansion aerodynamic window, compression aerodynamic window and vortex aerodynamic window. The area of these windows is approximately 3x3 cm^2. They all attain a specified cavity pressure of 0.1 atm. Moreover, they can operate mormally in a certain range deviating from the specified cavity pressure. The emission level of the beam produced after the beam passes through the window is used to appraise

the optical quality of the window. The divergence angle after the beam passes through the expansion window and vortex window is 1.47-1.70 times as large as the diffraction limit of the aperture but after the beam passes through the compression window the divergence angle is 2.06-2.13 times as large as the diffraction limit of the aperture. The minimum mass flow when using these windows takes the vortex window as the minimum, about 0.012-0.023 kg/sec · cm^2. These windows can be applied in the output windows of continuously operating high power aerodynamic lasers or electrically excited aerodynamic lasers.

Principles and Design

The window which we developed was aimed at the design of a continuous megawatt level aerodynamic laser and its typical cavity pressure is 0.1 atm. It is required that the aerodynamic window possess the function of being able to seal the optical cavity and not influence the quality of the output beam.

(1) The expansion aerodynamic window: it uses an expansion wave produced by supersonic airflow flowing around the exterior angle of refraction to seal the window. When the nozzle exit's static pressure and atmospheric pressure match, the static pressure behind the expansion wave and optical cavity match [2] (see Fig. 1).

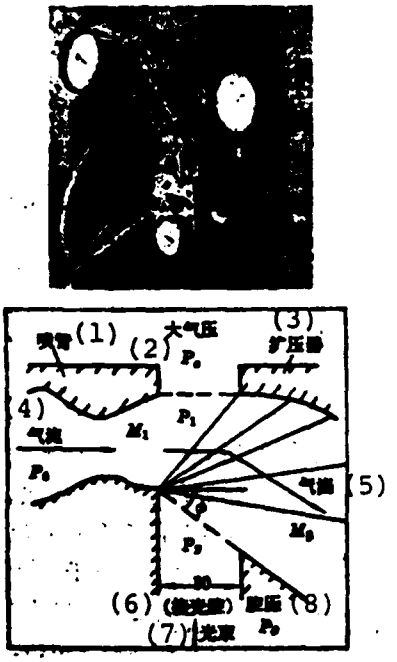

Fig. 1. Photograph and operating principle of expansion window.
Key: (1) Nozzle; (2) Atmospheric pressure; (3) Diffuser; (4) Airflow; (5) Airflow; (6) Connected to cavity; (7) Beam; (8) Cavity pressure.

The window dimensions are 30x34 mm^2, designed cavity pressure P_c=0.1 atm, nozzle exit Mach number M_1=1.8, and P_1=1 atm. The nozzle's supersonic velocity transition section is designed by the Atkin method, the initial expansion section is composed from the linear and throat area arc, and the subsonic velocity section is the simple arc. The nozzle type line makes boundary layer corrections. The designed expansion pressure ratio P_1/P_2= 10, M_2=3.3, and the corresponding airflow angle of refraction is 34.5°. When considering the influence of the low pressure turbulent flow shearing layer on one side, we take the geometric expansion angle ϕ =35°, the exhaust duct pressure curve section on one side uses a wave elimination method design, and the supersonic diffuser's throat section F*=1900 mm^2.

The experimentally observed shock wave system is the shock waves produced by the shearing layer and boundary layer. This type of shock cannot bring the sealed window aperture into effect and therefore this type of aerodynamic window is still an expansion aerodynamic window. It is different for the compression window which relies on the shock waves to seal the window aperture which will be discussed below.

(2) The compression aerodynamic window: it is a shock wave which is formed by the nozzle exit's supersonic airflow on the atmospheric side and is adjusted to the atmospheric pressure [2] as shown in Fig. 2.

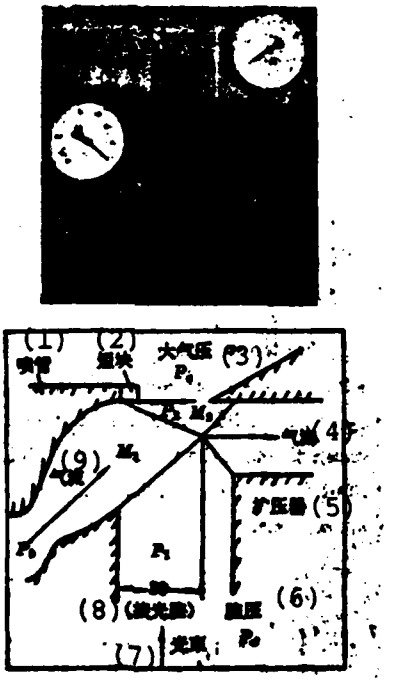

Fig. 2. Photograph and operating principle of compression window. Key: (1) Nozzle; (2) Short block; (3) Atmospheric pressure; (4) Airflow ; (5) Diffuser; (6) Cavity pressure; (7) Beam; (8) (Connected optical cavity; (9) Airflow.

The window dimensions are 30x22 mm^2, the designed cavity pressure P_c=0.1 atm, nozzle exit Mach number M_1=3.65, shock wave oblique angle β =54°, airflow angle of refraction θ =34°9', and the Mach number behind the wave M_2=1.408. The nozzle's supersonic velocity transition section uses the Atkin method for design, the throat line uses a cubic curve, and the subsonic velocity transition section uses the Weituoxinsiji curve. The nozzle type curve also makes boundary layer corrections. Nozzle throat height h*=3.3mm, nozzle exit height h=25.8mm, and the airflow passes through the section which is F*=960mm^2 and is exhausted by the exhaust duct.

(3) The vector aerodynamic window: this uses a vortex airflow centrifugal force produced by the supersonic velocity nozzle to attain a balanced air pressure difference inside and outside of the laser cavity. Moreover, a suitable nozzle exit Mach number is selected so that the outer pressure and atmospheric pressure match and the airflow's inner pressure and cavity pressure match [3], as shown in Fig. 3.

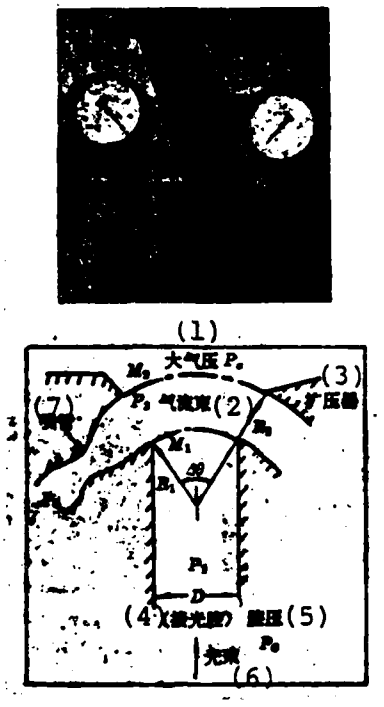

Fig. 3. Photograph and operating principle of vortex window.
Key: (1) Atmospheric pressure P_c; (2) Airflow beam; (3) Diffuser; (4) (Connected to optical cavity); (5) Cavity pressure; (6) Beam: (7) Nozzle.

The window dimensions are $30\text{x}30\text{mm}^2$, designed cavity pressure P_o=0.1 atm, airflow rotational angle $\Delta\theta$=60°, the nozzle's outer wall exit Mach number M_2=2.01 and M_2^*=1.63751. The nozzle's inner wall exit Mach number M_1=3.53, M_1^*=2.06927, the ideal airflow beam's inner side radius $R_1 = \frac{D}{2} / \sin\frac{\Delta\theta}{2}$=30mm, and the ideal airflow beam's outer side radius $R_2 = \frac{M_1^* \cdot R_1}{M_2^*}$=37.8mm. In order to attain the rotating airflow beam, it is necessary to cause the velocity change on the nozzle exit's plane to be in inverse ratio to the efflux curve radius [3]. It uses a 19.022° angle flat flow with a common convergent-divergent supersonic nozzle (its design

method is the same as that of the compression window) flowing into a vortex nozzle. The vortex nozzle is designed with a characteristic line method so that the airflow goes through different expansion on the inner and outer walls of this nozzle and the parameters of the nozzle exit reach a velocity distribution of $M^* \cdot R_i = k$ (constant). Because the rotation of the flow is a characteristic line or maintains a Mach wave on the nozzle exit plane, it can avoid strong shock waves. Nozzle height h=7.8mm, throat height h*=3.44mm and the boundary layer's single side correction quantity δ^*=0.28mm. After the airflow beam sweeps passed window angle $\Delta\theta$, it is exhausted by the exhaust duct which has an area of $F^*=1230mm^2$.

Flow Field Observations

We used the schlieren method for the three types of windows to observe and photograph the flow field flow patterns under various stagnation pressures. Fig. 4 is the flow patterns of several different typical operating conditions of the expansion window. We can see that following the decline of stagnation pressure P_o, the window aperture's high pressure side oblique shock wave deflects towards the upstream and the atmosphere leaks in.

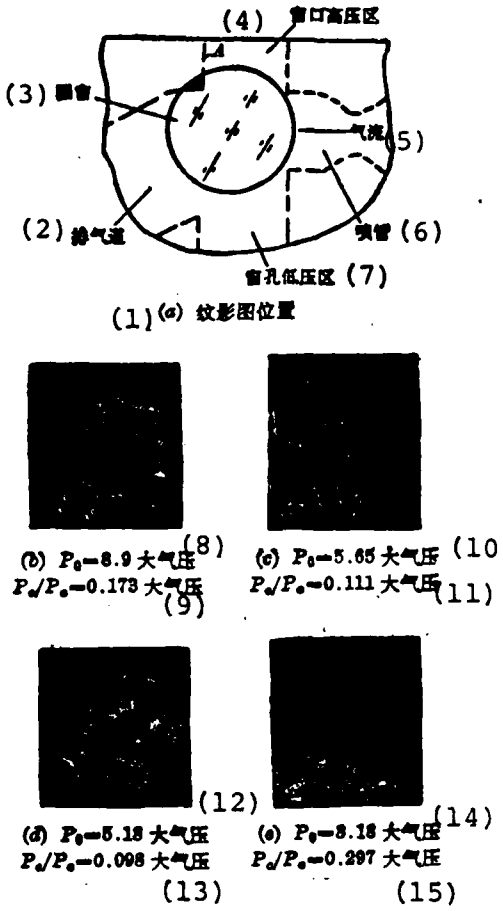

Fig. 4. Flow patterns of several typical operating conditions of the expansion window.
Key: (1) Schlieren chart position; (2) Exhaust line; (3) Circular window; (4) Window's high pressure area; (5) Airflow; (6) Nozzle; (7) Window aperture's low pressure area; (8) atm; (9) atm; (10) atm; (11) atm; (12) atm; (13) atm; (14) atm; (15) atm.

Fig. 5 is the flow patterns of several typical operating conditions of the compression window. We can clearly see a shock wave separated from the sealed window and atmosphere. We can also discover from the photos that the two oblique shock waves formed on the nozzle type line enter the window's flow field and seriously influence the optical quality of the window.

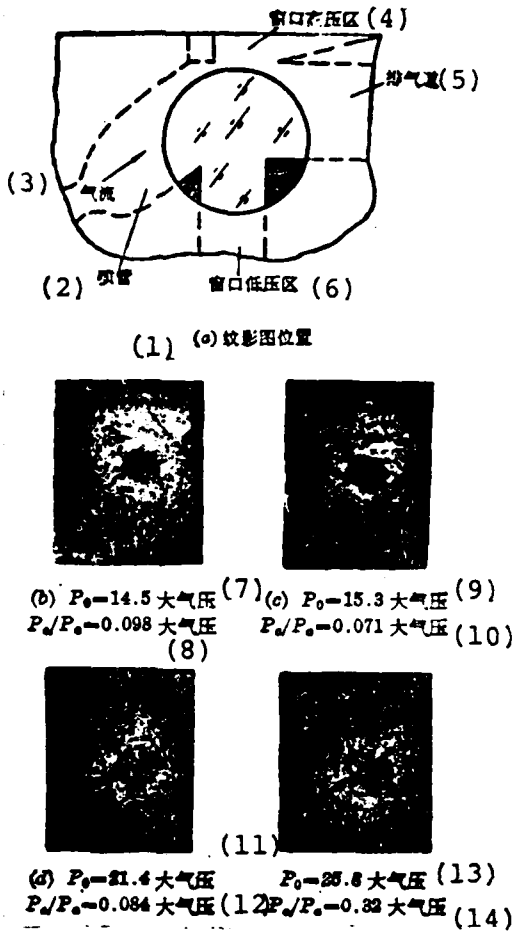

Fig. 5. Flow patterns of several typical operating conditions of the compression window.
Key: (1) Schlieren chart position; (2) Nozzle; (3) Airflow; (4) Window's high pressure area; (5) Exhaust duct; (6) Window's low pressure area; (7) atm; (8) atm; (9) atm; (10) atm; (11) atm; (12) atm; (13) atm; (14)atm.

Fig. 6 is the flow patterns of several different typical operating conditions of the vortex window. We can see in the flow field area near the nozzle exit the characteristic line area formed by the weak compression wave and weak expansion wave. We can also see from the photographs that when the stagnation pressure rises, because the nozzle exit pressure next to the atmospheric side is higher than the atmospheric pressure, under-expansion occurs.

Optical Performance

To determine the optical performance of the window, we used a helium-neon laser for the analog beam. During experiments, the beam passes through a series of neutral filters (the aim is to avoid the base plate emulsion blackness saturation and production of nonlinear errors). After beam expansion by the beam expander it passes through the window, is focused on the negative by a lens with a focal distance of f=5 meters, uses a 9n type microphotometer to measure the Gaussian distribution of the light spot, and calculates the distribution of the light energy following the light spot radius and the divergence angle of the beam. To avoid the influence of square aperture diffraction on the light spot intensity measurement, we used a circular aperture diaphragm ϕ d.

Fig. 7 is light spot photographs taken when the expansion window, compression window and vortex window were operating close to the design operated cavity pressure.

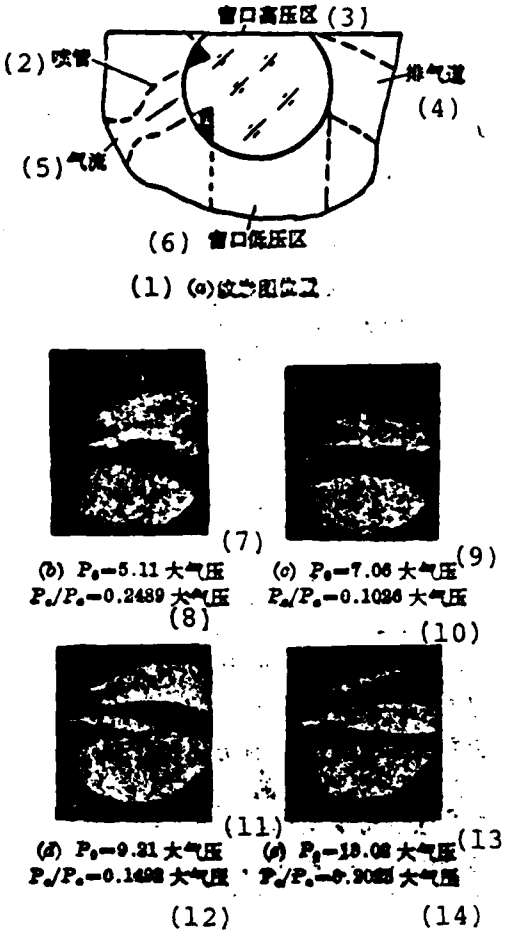

Fig. 6. Flow patterns of several typical operating conditions of the vortex window.
Key: (1) Schlieren chart position; (2) Nozzle; (3) Window's high pressure; (4) Exhaust duct; (5) Airflow; (6) Window's low pressure area; (7) atm; (8) atm; (9) atm; (10) atm; (11) atm; (12) atm; (13) atm; (14) atm.

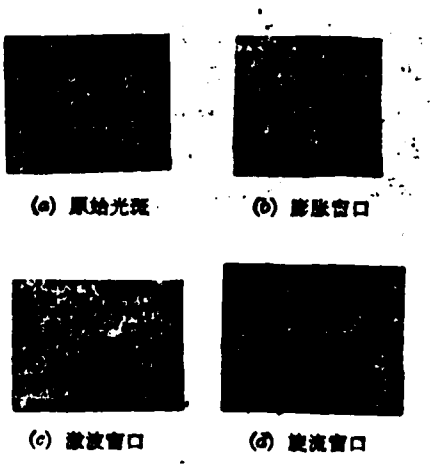

Fig. 7. The distant field light spots after the beam passes through the window (operating conditions: cavity pressure $P_c/P_a \approx 0.1$ atm).

Key: (a) Original spot; (b) Expansion window; (c) Compression window; (d) Vortex window.

Fig. 8 is the corresponding normalized distant field intensity which changes with light spot radius R.

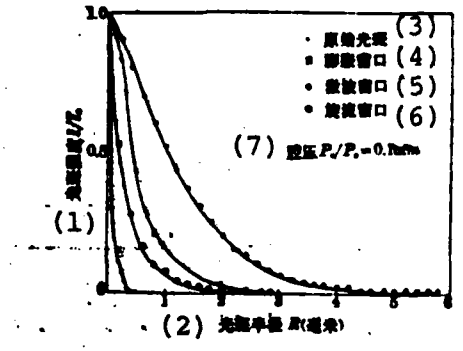

Fig. 8. Distribution (λ=6328Å) of distant field intensity following light spot radius R.

Key: (1) Light spot intensity I/T; (2) Light spot radius R (mm);

(3) Original light spot; (4) Expansion window; (5) Compression window; (6) Vortex window; (7) Cavity pressure.

Fig. 9 is the corresponding energy distribution curve. When there is an 80% beam concentration of energy and the radius is light spot radius R, we find that beam divergence angle $\theta_{divergent}=tg^{-1}\frac{R}{f}$ and the ideal parallel beam's diffraction limit angle $\theta_{diffraction}=2x1.22x\frac{\lambda}{d}$ are comparable.

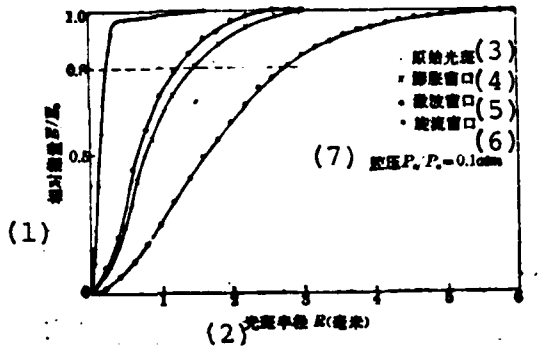

Fig. 9. Light energy distribution of light spots (λ =6328Å).
Key: (1) Relative energy E/E_o ; (2) Light spot radius R (mm); (3) Original light spot; (4) Expansion window; (5) Compression window; (6) Vortex window; (7) Cavity pressure.

Fig. 10 shows the changes of the relative beam divergence angle $\theta_{divergent}/\theta_{diffraction}$ of the three types of windows under different cavity pressure operating conditions.

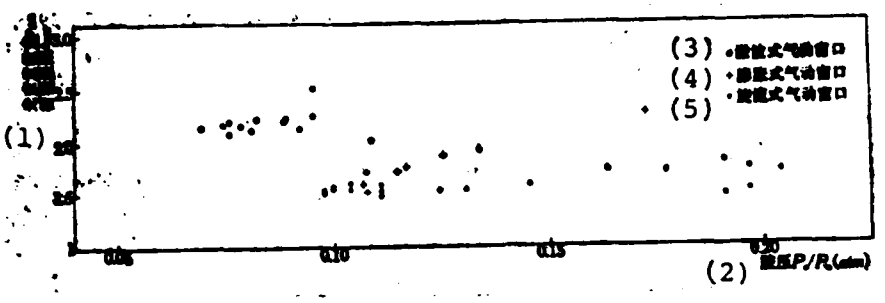

Fig. 10. Relationship of the divergence angle of the beam passing through the aerodynamic window following the cavity pressure.

Key: (1) $\frac{\text{beam divergence angle } \theta_{divergent}}{\text{diffraction limit } \theta_{diffraction}}$; (2) Cavity pressure; (3) Compression aerodynamic window; (4) Expansion aerodynamic window; (5) Vortex aerodynamic window.

Results show that the window's optical quality and operating conditions are related. When the expansion window's corresponding cavity pressure P_c/P_a=0.095-0.125 atm, the divergence angle after the beam passes through the window is 1.5-1.7 times as large as the diffraction limit. When cavity pressure $P_c/P_a > 0.134$ atm, the output beam has serious divergence and reaches to over 2.3 times as large as the diffraction limit. Moreover, following the increase of P_o, the beam directionality tends to worsen. This is because following the increase of P_o, the more formidable the airflow's external refraction, when the airflow circulates around the downstream window aperture wall, the further the produced detached shock from the wall surface and the more serious the leakage flow. As a result, the beam directionality rapidly worsens. When the vortex window is in the cavity pressure P_c/P_o=0.098-0.146 atm range, after the beam passes through the aerodynamic window the divergence angle is 1.47-1.59 times as large as the diffraction limit. The divergence angle enlarges with the increase of the stagnation pressure. In the cavity

pressure range of P_c/P_o=0.069-0.15 atm, after the beam passes through the aerodynamic window the divergence angle light spot is 2.06-2.13 times as large as the diffraction limit. The divergence angle enlarges with the increase of the stagnation pressure.

Conclusions

(1) The three types of windows all satisfy operating condition P_c/P_o=0.1 atm . Moreover, we can use the method of regulating the stagnation pressure so that the window operates steadily in a certain range deviating from the designed conditions. This possesses certain suitable capabilities for the optical cavity pressure.

(2) The optical performance is better when using the expansion window and vortex window and poor when using the compression window.

(3) In using these windows, the mass flow is minimum when using the vortex window. Therefore, when in use, the required air source equipment is small and economy is good. At the same time, the operation of the expansion window and vortex window is convenient and if we use smaller stagnation pressure they can operate normally. The operating pressure of the compression window is then too large.

(4) After the performance and structure of the vortex window and expansion window are further improved, they can be used for the output windows of aerodynamic lasers and electrically excited lasers.

(5) The major performances are listed in the following table.

(1) 性能	(6) 窗口形式		
	(7) 膨胀窗口	(8) 激波窗口	(9) 漩流窗口
(2) 工作腔压范围(大气压)	0.095~0.125	0.069~0.15	0.098~0.146
(3) 光束发散角(衍射极限的倍数)	1.5~1.7	2.06~2.13	1.47~1.59
(4) 耗气量(千克/秒·厘米^2)	0.051~0.069	0.051~0.061	0.012~0.023
(5) 运转滞止压力(大气压)	4.8	15.2	5.3

Key: (1) Performance; (2) Operating cavity pressure range (atm); (3) Beam's divergence angle (multiple of diffraction limit); (4) Mass flow (kg/sec·cm^2); (5) Operating stagnation pressure (atm); (6) Window type; (7) Expansion window; (8) Compression window; (9) Vortex window.

References

[1] Ethan Hoag et al.; Appl. Opt., 1974, 13, No. 8, 1959.

[2] E.M. Parmenfier; AIAA J., 1973, 11, No. 7, 943.

[3] R.N. Guile; AIAA-75-122, 1975.


DATE
ILME